OFFPRINT

Light polarons and bipolarons for a highly inhomogeneous electron-boson coupling

M. Berciu and G. A. Sawatzky

Please visit the new website
www.epljournal.org

TAKE A LOOK AT THE NEW EPL

Europhysics Letters (EPL) has a new online home at
www.epljournal.org

Light polarons and bipolarons for a highly inhomogeneous electron-boson coupling

M. BERCIU and G. A. SAWATZKY

Department of Physics and Astronomy, University of British Columbia - Vancouver, BC V6T 1Z1, Canada

Abstract – We derive the exact polaron and bipolaron Green's functions for a model with a highly inhomogeneous electron-boson coupling $g_{\vec{q}} \propto \delta_{\vec{q},\vec{Q}}$, where $\vec{Q} = \frac{\pi}{a}(1, \ldots, 1)$. While the polaron ground-state energy and quasiparticle weight are similar to those of the Holstein polaron with equal effective coupling, the polaron dispersion is very different. Unlike that of a Holstein polaron, which is monotonically increasing with the polaron momentum, the polaron dispersion in this case is folded inside the Brillouin zone. For strong coupling, the polaron and bipolaron effective masses increase *linearly* with the effective coupling and exhibit no isotope effect, as opposed to an *exponential* increase and a strong isotope effect, in the Holstein model. As a result, this model exhibits *strongly bound* yet *light bipolarons* at strong couplings. Generalizations are discussed.

Introduction. – Exact solutions for interacting systems are of considerable interest in condensed matter physics, even for models simplified to a large degree. Such models can describe non-trivial physics, and exact solutions provide unique insight into regimes not accessible by perturbation theory or other simple analytical approximations. Such exact solutions can also be used as benchmarks for testing of numerical algorithms developed for simulations of more general models.

The problem we focus on in this letter are the effective properties of dressed single particles and pairs of particles, due to interactions with bosons. Such interactions are ubiquitous in complex materials, the bosons being phonons, magnons and/or orbitronic degrees of freedom. The general electron-boson interaction for electrons on a N-site lattice in d-dimensions is given by [1]

$$\hat{V} = \sum_{\vec{k},\sigma,\vec{q}} \frac{g_{\vec{k},\vec{q}}}{\sqrt{N}} c^{\dagger}_{\vec{k}-\vec{q},\sigma} c_{\vec{k}\sigma} \left(b^{\dagger}_{\vec{q}} + b_{-\vec{q}} \right),$$

where $c_{\vec{k}\sigma}$ and $b_{\vec{q}}$ are electron and boson annihilation operators, and momenta sums are over the corresponding Brillouin zone (BZ). Well-known examples of such interactions are described by the Holstein model ($g_{\vec{k},\vec{q}} = g$) [2,3] and by the Fröhlich model ($g_{\vec{k},\vec{q}} \sim 1/q$) [4]. In these cases, the coupling is either a constant or (apart from the $q = 0$ region) a rather slowly-varying function of $\vec{q}$.

However, there are also systems where $g_{\vec{k},\vec{q}}$ is peaked in the "corner" of the Brillouin zone. Examples include coupling to phonon breathing modes, which is essential in describing the behavior of Bi oxide superconductors [5,6] and may also play an important role in cuprates [7–10]; to antiferromagnons, *e.g.* in underdoped cuprates [11] and in antiferromagnetically ordered phases of manganites [12]; and to combined spin and orbitron degrees of freedom in certain manganites [13]. Graphene also exhibits strong coupling to (its corner) K-point optical phonons [14], which is promising for the possibility of engineering such models using cold atoms trapped in optical lattices [15].

In this work, we derive exact finite-temperature Green's functions for dressed particles (polarons) and pairs of dressed particles (bipolarons) for a simple, highly inhomogeneous coupling (HIC) which assumes interactions only with the boson of momentum $\vec{Q} = \frac{\pi}{a}(1,..,1)$. All other bosons are assumed to be irrelevant. This allows us to calculate exactly various properties of the polarons and bipolarons, such as effective masses, binding energies, etc. We can also contrast their behavior with that of Holstein polarons and bipolarons, to highlight the main differences due to such a HIC model as opposed to a model with a (quasi)homogeneous coupling. Several possible generalizations are also briefly considered.

The model. – The HIC model that we study is

$$\mathcal{H} = \sum_{\vec{k}\sigma} \epsilon_{\vec{k}} c^\dagger_{\vec{k}\sigma} c_{\vec{k}\sigma} + \Omega b^\dagger_{\vec{Q}} b_{\vec{Q}} + g \sum_{\vec{k}} c^\dagger_{\vec{k}-\vec{Q},\sigma} c_{\vec{k}\sigma} \left(b^\dagger_{\vec{Q}} + b_{\vec{Q}} \right). \tag{1}$$

Here, $\epsilon_{\vec{k}} = -2t \sum_{i=1}^d \cos(k_i a)$ is the free electron energy corresponding to nearest-neighbor hoping on a d-dimensional simple cubic lattice of lattice constant a (generalization to longer-range hopping is trivial). Ω is the energy of the bosons (we set $\hbar = 1$ throughout this work) and g characterizes the coupling to the bosons of momentum $\vec{Q}$. While the model is rather unphysical, as it implies an infinite-range coupling in real space, its exact solutions suggest useful conclusions about models with long but finite-range couplings, as discussed below. Furthermore, for more realistic models, weak coupling to other bosons can be added perturbatively at a second stage.

Methodology. – The finite-temperature polaron Green's function is defined as [1]

$$G(\vec{k}, \tau) = -i\Theta(\tau) Tr\left(\hat{\rho} c_{\vec{k}}(\tau) c^\dagger_{\vec{k}} \right). \tag{2}$$

The trace is over all zero-electron eigenstates $|n\rangle = \frac{1}{\sqrt{n!}} (b^\dagger_{\vec{Q}})^n |0\rangle$ with energies $\mathcal{H}|n\rangle = n\Omega|n\rangle$. The equilibrium density matrix is $\hat{\rho} = \frac{1}{Z} e^{-\beta\mathcal{H}}$ with the corresponding partition function $Z = Tr\hat{\rho} = (1 - e^{-\beta\Omega})^{-1}$ and $\beta = (k_B T)^{-1}$. Finally, $\Theta(\tau)$ is the step function and $c_{\vec{k}}(\tau) = e^{i\mathcal{H}\tau} c_{\vec{k}} e^{-i\mathcal{H}\tau}$. In the frequency domain, this becomes equal to

$$G(\vec{k}, \omega) = \sum_{n=0}^\infty \frac{e^{-n\beta\Omega}}{n!Z} G_{nn}(\vec{k}, \omega + n\Omega), \tag{3}$$

where we introduce the generalized Green's function:

$$G_{nm}(\vec{k}, \omega) = \langle 0 | b^n_{\vec{Q}} c_{\vec{k}} \hat{G}(\omega) c^\dagger_{\vec{k}+(n-m)\vec{Q}} (b^\dagger_{\vec{Q}})^m | 0 \rangle, \tag{4}$$

with the usual resolvent $\hat{G}(\omega) = (\omega - \mathcal{H} + i\eta)^{-1}$, and $\eta > 0$ an infinitesimally small real number. These Green's functions can be calculated by applying repeatedly Dyson's identity $\hat{G}(\omega) = \hat{G}_0(\omega) + \hat{G}(\omega)\hat{V}\hat{G}_0(\omega)$, where $\hat{G}_0(\omega) = (\omega - \mathcal{H}_0 + i\eta)^{-1}$ corresponds to the non-interacting Hamiltonian $\mathcal{H}_0 = \mathcal{H} - \hat{V}$, leading to the recurrence relations:

$$G_{nm} = g_{nm} \left(\delta_{n,m} n! + mg G_{n,m-1} + g G_{n,m+1} \right), \tag{5}$$

where, for simplicity, the $(\vec{k}, \omega)$-dependence is not written explicitly and we use the shorthand notation

$$g_{nm} \equiv g_{nm}(\vec{k}, \omega) = G_0(\vec{k} + (n-m)\vec{Q}, \omega - m\Omega), \tag{6}$$

with $G_0(\vec{k}, \omega) = (\omega - \epsilon_{\vec{k}} + i\eta)^{-1}$ being the non-interacting single electron Green's function. These equations are solved in terms of continued fractions [16], and we find

$$G(\vec{k}, \omega) = \sum_{n=0}^\infty \frac{e^{-n\beta\Omega}\left(1 - e^{-\beta\Omega}\right)}{\omega - \epsilon_{\vec{k}} - A_n(\vec{k}, \omega) - B_n(\vec{k}, \omega) + i\eta}, \tag{7}$$

where (see eq. (6) for definition of $g_{nm}(\vec{k}, \omega)$)

$$A_n(\vec{k}, \omega) = \cfrac{ng^2 g_{0,-1}}{1 - \cfrac{(n-1)g^2 g_{0,-1}g_{0,-2}}{1 - \cfrac{(n-2)g^2 g_{0,-2}g_{0,-3}}{\cdots}}}, \tag{8}$$

$$B_n(\vec{k}, \omega) = \cfrac{(n+1)g^2 g_{0,1}}{1 - \cfrac{(n+2)g^2 g_{0,1}g_{0,2}}{1 - \cfrac{(n+3)g^2 g_{0,2}g_{0,3}}{\cdots}}} \tag{9}$$

are finite, respectively infinite continued fractions. If the coupling depends on the incoming electron's momentum $\vec{k}$, one simply has to replace $g^2 \to |g_{\vec{k}}|^2$. For $T = 0$ only the $n = 0$ term is finite, therefore $B_0(\vec{k}, \omega)$ is the polaron self-energy, with explicit and non-trivial $\vec{k}$-dependence.

Similarly, the bipolaron Green's function in the singlet sector is defined as

$$\mathcal{G}(\vec{K}_1\vec{K}_2, \vec{k}_1\vec{k}_2; \tau) = -i\Theta(\tau) Tr\left(\hat{\rho} c_{\vec{K}_2\downarrow}(\tau) c_{\vec{K}_1\uparrow}(\tau) c^\dagger_{\vec{k}_1\uparrow} c^\dagger_{\vec{k}_2\downarrow} \right).$$

Let $\vec{k}^{(+)} = \vec{k}$, $\vec{k}^{(-)} = \vec{k} - \vec{Q}$, and define the generalized two-particle Green's functions:

$$\mathcal{G}^{\pm\pm}_{nm}(\vec{K}_1\vec{K}_2, \vec{k}_1\vec{k}_2; \omega) = \\ \langle 0 | b^n_{\vec{Q}} c_{\vec{K}_2\downarrow} c_{\vec{K}_1\uparrow} \hat{G}(\omega) c^\dagger_{\vec{k}_1^{(\pm)}\uparrow} c^\dagger_{\vec{k}_2^{(\pm)}\downarrow} (b^\dagger_{\vec{Q}})^m | 0 \rangle.$$

In terms of these, after a Fourier transform to the frequency domain, the bipolaron Green's function equals

$$\mathcal{G}(\vec{K}_1\vec{K}_2, \vec{k}_1\vec{k}_2; \omega) = \sum_{n=0}^\infty \frac{e^{-n\beta\Omega}}{Zn!} \mathcal{G}^{++}_{nn}(\vec{K}_1\vec{K}_2, \vec{k}_1\vec{k}_2; \omega + n\Omega). \tag{10}$$

The recurrence relations for $\mathcal{G}^{\pm\pm}_{nm}(\vec{K}_1\vec{K}_2, \vec{k}_1\vec{k}_2; \omega)$ are generated as before, using Dyson's equation repeatedly. They are found to be given by

$$\mathcal{G}^{++}_{nm} = \mathcal{G}_0(\vec{k}_1, \vec{k}_2, \omega - m\Omega) \left[\delta_{n,m} n! \delta_{\vec{K}_1,\vec{k}_1} \delta_{\vec{K}_2,\vec{k}_2} \right. \\ \left. + mg\left(\mathcal{G}^{-+}_{n,m-1} + \mathcal{G}^{+-}_{n,m-1} \right) + g\left(\mathcal{G}^{-+}_{n,m+1} + \mathcal{G}^{+-}_{n,m+1} \right) \right],$$

$$\mathcal{G}^{--}_{nm} = \mathcal{G}_0(\vec{k}_1^{(-)}, \vec{k}_2^{(-)}, \omega - m\Omega) \left[\delta_{n,m} n! \delta_{\vec{K}_1,\vec{k}_1^{(-)}} \delta_{\vec{K}_2,\vec{k}_2^{(-)}} \right. \\ \left. + mg\left(\mathcal{G}^{-+}_{n,m-1} + \mathcal{G}^{+-}_{n,m-1} \right) + g\left(\mathcal{G}^{-+}_{n,m+1} + \mathcal{G}^{+-}_{n,m+1} \right) \right],$$

$$\mathcal{G}^{+-}_{nm} = \mathcal{G}_0(\vec{k}_1, \vec{k}_2 - \vec{Q}, \omega - m\Omega) \\ \times \left[mg\left(\mathcal{G}^{++}_{n,m-1} + \mathcal{G}^{--}_{n,m-1} \right) + g\left(\mathcal{G}^{++}_{n,m+1} + \mathcal{G}^{--}_{n,m+1} \right) \right]$$

and finally

$$\mathcal{G}^{-+}_{nm} = \mathcal{G}_0(\vec{k}_1 - \vec{Q}, \vec{k}_2, \omega - m\Omega) \\ \times \left[mg\left(\mathcal{G}^{++}_{n,m-1} + \mathcal{G}^{--}_{n,m-1} \right) + g\left(\mathcal{G}^{++}_{n,m+1} + \mathcal{G}^{--}_{n,m+1} \right) \right],$$

where we did not write the arguments $(\vec{K}_1\vec{K}_2, \vec{k}_1\vec{k}_2; \omega)$ explicitly for simplicity of notation, but dependence on these is implicitly assumed. Also, $\mathcal{G}_0(\vec{k}_1, \vec{k}_2, \omega) = (\omega - \epsilon_{\vec{k}_1} - \epsilon_{\vec{k}_2} + i\eta)^{-1}$ are the free two-electron Green's functions.

In order to solve this infinite system of coupled recurrence equations, we define

$$F_{nm} \equiv \begin{cases} \mathcal{G}_{nm}^{++} + \mathcal{G}_{nm}^{--}, & \text{if } n-m \text{ is even,} \\ \mathcal{G}_{nm}^{+-} + \mathcal{G}_{nm}^{-+}, & \text{if } n-m \text{ is odd,} \end{cases} \quad (11)$$

and

$$\tilde{g}_{nm} \equiv \begin{cases} g_+(\vec{k}_1, \vec{k}_2, \omega - m\Omega), & \text{if } n-m \text{ is even,} \\ g_-(\vec{k}_1, \vec{k}_2, \omega - m\Omega), & \text{if } n-m \text{ is odd,} \end{cases} \quad (12)$$

where again, dependence on $(\vec{K}_1\vec{K}_2, \vec{k}_1\vec{k}_2; \omega)$ is implicitly assumed, and we also introduce

$$g_+(\vec{k}_1, \vec{k}_2, \omega) = \mathcal{G}_0(\vec{k}_1, \vec{k}_2, \omega) + \mathcal{G}_0(\vec{k}_1 - \vec{Q}, \vec{k}_2 - \vec{Q}, \omega)$$

and

$$g_-(\vec{k}_1, \vec{k}_2, \omega) = \mathcal{G}_0(\vec{k}_1 - \vec{Q}, \vec{k}_2, \omega) + \mathcal{G}_0(\vec{k}_1, \vec{k}_2 - \vec{Q}, \omega).$$

Then, the four original recurrence relations reduce to one similar to eq. (5), namely

$$F_{nm} = \delta_{n,m} n! f_n + g\tilde{g}_{nm} \left(m F_{n,m-1} + F_{n,m+1} \right),$$

where

$$f_n \equiv \mathcal{G}_0(\vec{K}_1, \vec{K}_2, \omega - n\Omega)(\delta_{\vec{K}_1, \vec{k}_1} \delta_{\vec{K}_2, \vec{k}_2} + \delta_{\vec{K}_1, \vec{k}_1^{(-)}} \delta_{\vec{K}_2, \vec{k}_2^{(-)}}).$$

This is again solved in terms of continued fractions, after which the various $\mathcal{G}_{nm}^{(\pm, \pm)}$ functions can be found from their original recurrence equations, which depend only on the F_{nm} combinations (see eq. (11)). In particular, the expressions needed in eq. (10) are found to be given by

$$\frac{\mathcal{G}_{nn}^{++}(\vec{K}_1\vec{K}_2, \vec{k}_1\vec{k}_2; \omega + n\Omega)}{n!} = \delta_{\vec{K}_1, \vec{k}_1} \delta_{\vec{K}_2, \vec{k}_2} \mathcal{G}_0(\vec{k}_1, \vec{k}_2, \omega)$$
$$+ \left(\delta_{\vec{K}_1, \vec{k}_1} \delta_{\vec{K}_2, \vec{k}_2} + \delta_{\vec{K}_1, \vec{k}_1^{(-)}} \delta_{\vec{K}_2, \vec{k}_2^{(-)}} \right) \mathcal{G}_0(\vec{K}_1, \vec{K}_2, \omega)$$
$$\times \frac{\left[\tilde{A}_n(\vec{k}_1, \vec{k}_2, \omega) + \tilde{B}_n(\vec{k}_1, \vec{k}_2, \omega) \right] \mathcal{G}_0(\vec{k}_1, \vec{k}_2, \omega)}{1 - g_+(\vec{k}_1, \vec{k}_2, \omega) \left[\tilde{A}_n(\vec{k}_1, \vec{k}_2, \omega) + \tilde{B}_n(\vec{k}_1, \vec{k}_2, \omega) \right]},$$

where $\tilde{A}_n(\vec{k}_1, \vec{k}_2, \omega)$ and $\tilde{B}_n(\vec{k}_1, \vec{k}_2, \omega)$ have the same expressions as in eqs. (8) and (9), but with $\tilde{g}_{nm}(\vec{k}_1, \vec{k}_2, \omega)$ of eq. (12) replacing g_{nm}. These expressions show that the momenta of the two electrons are either unchanged or differ by $\vec{Q}$, if even/odd numbers of bosons are exchanged by the pair. Note that all other Green's functions are also known, allowing one to calculate exactly any quantity of interest. Here we continue to focus only on the polaron and bipolaron Green's functions, eqs. (7) and (10).

From the Lehmann representation we know that poles of the $T=0$ polaron Green's function mark the spectrum of the polaron [1]. We can thus find $E_P(\vec{k})$, the lowest polaron eigenstate for a given $\vec{k}$, and the polaron effective mass, $m_P = (\lim_{k\to 0} \mathrm{d}^2 E_P(\vec{k})/\mathrm{d}k^2)^{-1}$ from its second derivative at the center of the BZ. The residues
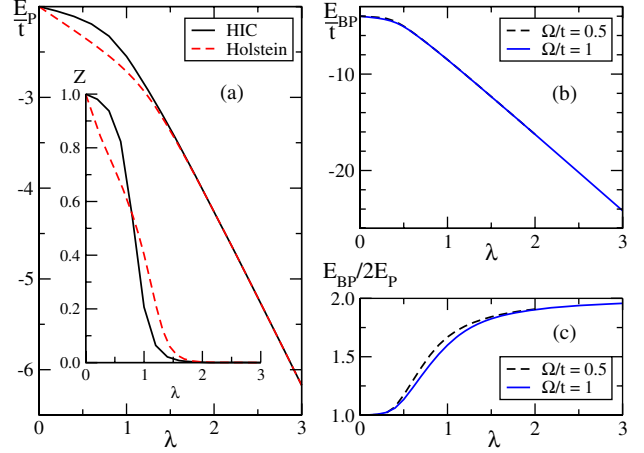

Fig. 1: (Color online) Results for $d=1$. (a) Polaron GS energy and (in inset) qp weight $vs.$ $\lambda = g^2/(2dt\Omega)$, for $\Omega = 0.5t$. (b) Bipolaron GS energy, for $\Omega/t = 0.5$ and 1 (the two curves are practically indistinguishable). (c) Ratio of bipolaron GS energy to twice the polaron GS energy.

are the quasiparticle (qp) weights $Z(k) = |\langle \phi(\vec{k}) | c_{\vec{k}}^\dagger | 0 \rangle|^2$, with $|\phi(\vec{k})\rangle$ the one-electron eigenstate of energy $E_P(\vec{k})$. The spectral weight $A(\vec{k}, \omega) = -\frac{1}{\pi} \mathrm{Im} G(\vec{k}, \omega)$ is also a quantity of interest, since it is directly comparable against angle-resolved photoemission experiments (ARPES) [17]. Similarly, we can find the lowest energy $E_{BP}(\vec{k}_1, \vec{k}_2)$ for a bipolaron, its effective total mass $m_{BP} = 4(\lim_{k\to 0} \mathrm{d}^2 E_{BP}(\vec{k}, \vec{k})/\mathrm{d}k^2)^{-1}$, binding energies $E_{BP}(\vec{k}_1, \vec{k}_2) - \min_{\vec{q}}[E_P(\vec{k}_1 + \vec{q}) + E_P(\vec{k}_2 - \vec{q})]$, etc.

Results and discussion. – In this section we present typical one- and two-dimensional results and discuss their significance. The results for the HIC polaron are compared with those for the Holstein polaron, obtained with the momentum-average approximation [18,19]. We use the same g in both cases; this gives equal polaron ground-state (GS) energy in the impurity limit $E_P|_{\epsilon_k=0} = -g^2/\Omega$, and thus equal effective coupling $\lambda = g^2/(2dt\Omega)$ [19].

The polaron GS energies $E_P(0) \equiv E_P$ and qp weights are rather similar for the two models, as shown in fig. 1(a). This holds for a wide range of Ω/t values, and seems to suggests that the crossover from a large polaron (at weak coupling) to a small polaron (at strong coupling) is rather insensitive to the degree of inhomogeneity of the electron-phonon coupling. As discussed below, this quantitative agreement is somewhat misleading, because the nature of the polaron cloud in the strong-coupling limit is qualitatively different in the two models, even though their energies and qp weights are very comparable.

Figure 1(b) shows the bipolaron GS energy $E_{BP}(0,0) \equiv E_{BP}$. As expected, in the strong coupling limit $E_{BP} \to 4E_P$, since here bipolarons are strongly bound on-site singlets, with a binding energy of $E_{BP} - 2E_P \sim -2g^2/\Omega$. $E_{BP}/2E_P$ is shown in fig. 1(c). It is unity for $\lambda \to 0$, because here the phonon-mediated polaron-polaron
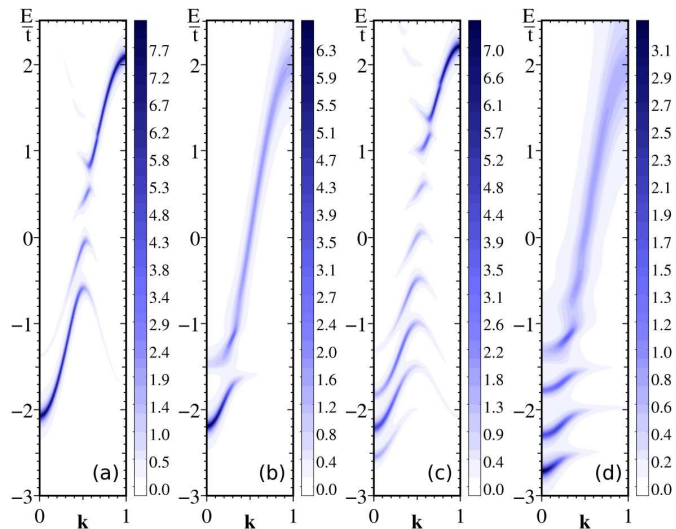
Fig. 2: (Color online) $T=0$, 1D polaron spectral weight $A(k,\omega)$. $t=1$, $\Omega=0.5$, $\eta=0.04$, $\lambda=0.3$ (a and b), $\lambda=1$ (c and d). HIC polaron (a and c) *vs.* Holstein polaron (b and d).
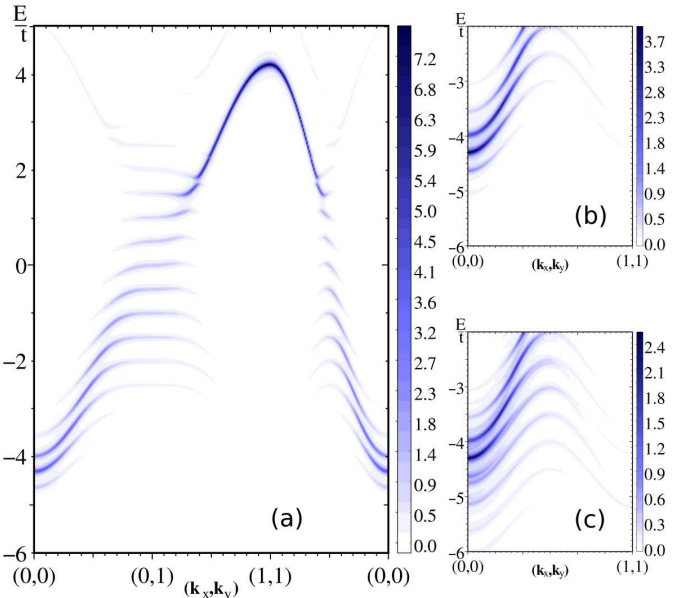

Fig. 3: (Color online) 2D HIC polaron spectral weight $A(\vec{k},\omega)$ along several cuts in the Brillouin zone, for $t=1$, $\Omega=0.5$, $\lambda=1$, $\eta=0.04$, and $T/\Omega=0$ (a and b), respectively, $T/\Omega=2$ (c). Note that the intensity scale is different for each panel.

interactions vanish, and it asymptotically goes to 2 as $\lambda \to \infty$. These conclusions also hold for all $d>1$.

While the GS energy is not very sensitive to the degree of inhomogeneity of the coupling, the higher-energy spectrum is. In fig. 2 we compare spectral weights of HIC and Holstein 1D polarons. For the Holstein polaron, the free electron state $c_{\vec{k}}^{\dagger}|0\rangle$ mixes with the continuums of all possible electron-plus-phonons states $c_{\vec{k}-\vec{q}_1}^{\dagger} b_{\vec{q}_1}^{\dagger}|0\rangle$, $c_{\vec{k}-\vec{q}_1-\vec{q}_2}^{\dagger} b_{\vec{q}_1}^{\dagger} b_{\vec{q}_2}^{\dagger}|0\rangle,\ldots$ for all values $\vec{q}_1$, $\vec{q}_2 \ldots$ As a result, a continuum appears at Ω above the GS energy [20], *i.e.* the self-energy acquires a finite imaginary part and the features are broadened and incoherent. Below this continuum there is a coherent qp state (the polaron band), whose energy increases *monotonically* with k while its qp weight decreases as $k \to \pi$ [19,21].

For the HIC polaron, the free electron state $c_{\vec{k}}^{\dagger}|0\rangle$ mixes only with the discrete set of states $c_{\vec{k}-\vec{Q}}^{\dagger} b_{\vec{Q}}^{\dagger}|0\rangle$, $c_{\vec{k}}^{\dagger}(b_{\vec{Q}}^{\dagger})^2|0\rangle,\ldots$ and therefore all the high-energy states remain coherent qp states, with infinite lifetimes (of course, weak coupling to other phonons would lead to a finite but long lifetime). Moreover, the HIC polaron dispersion is *doubly-folded*, as if the unit cell is doubled (the reason for this is discussed below). Note that this folding is clearly visible even at very weak couplings, as shown in fig. 2(a). Similar folding for the HIC spectrum is observed in all dimensions, as shown for $d=2$ in fig. 3(a). It becomes even more apparent at finite temperatures, as illustrated by the comparison between figs. 3(b) and 3(c). This, and the general behavior at finite T can be understood from the Lehmann representation of eq. (3):

$$G(\vec{k},\omega) = \sum_{n=0}^{\infty} \frac{e^{-n\beta\Omega}}{n!Z} \sum_{\alpha} \frac{|\langle\phi_\alpha(\vec{k})|c_k^{\dagger}(b_{\vec{Q}}^{\dagger})^n|0\rangle|^2}{\omega + n\Omega - E_\alpha(\vec{k}) + i\eta},$$

where $|\phi_\alpha(\vec{k})\rangle$ is a complete set of polaron eigenstates with momentum $\vec{k}$: $\mathcal{H}|\phi_\alpha(\vec{k})\rangle = E_\alpha(\vec{k})|\phi_\alpha(\vec{k})\rangle$ (α is the set of appropriate quantum numbers, besides the total momentum $\vec{k}$). At $T=0$ only the contribution from $n=0$ is finite. This equation shows that at finite-T satellite peaks appear due to $n \neq 0$ contributions, and are shifted by multiples of Ω from the $T=0$ energies. The associated weights (residues) are also different from those at $T=0$, since they now measure overlaps between the true eigenstates and states with different numbers n of phonons. This is the reason why some weights become larger as $\vec{k}$ approaches the Brillouin zone boundaries, making the "folding" more clearly visible. Because the appearance of these satellites peaks with changed weights is the only consequence of considering finite temperatures, in the rest we continue to discuss $T=0$ behavior and results.

To begin to understand the origin of this "folding", we use standard perturbation theory in the strong-coupling limit. We find the lowest HIC polaron energy to be given by

$$E_P(\vec{k}) = -\frac{g^2}{\Omega} + \epsilon_{\vec{k}} e^{-\frac{2g^2}{\Omega^2}} - \epsilon_{\vec{k}}^2 \frac{\Omega}{4g^2} + \ldots \qquad (13)$$

The third term dominates the dispersion for large λ, and is clearly responsible for the apparent band folding. However note that the translational symmetry is not broken: for any finite λ, the full Brillouin zone needs to be used because of the linear $\epsilon_{\vec{k}}$ term and higher-order terms that preserve it. This insures that the "folding" is not perfect, as indeed observed for weak couplings in fig. 2(a). Of course, to properly describe that case one needs to either go to a much higher order in the perturbational expansion
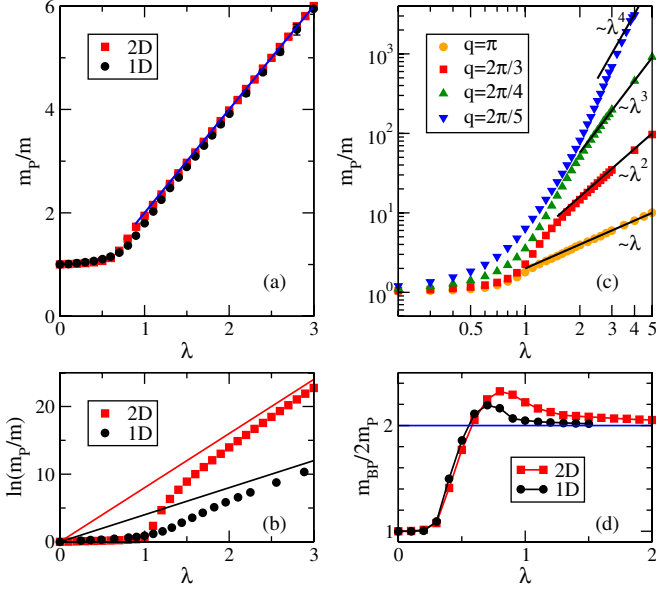
Fig. 4: (Color online) (a) HIC polaron effective mass for $d=1$ (circles) and $d=2$ (squares) and asymptotic value $m_P/m = 2\lambda$ (straight line). (b) Same for Holstein polaron. Here, asymptotic values are $\ln(m_P/m) = 2dt\lambda/\Omega$. (c) HIC polaron effective mass for $d=1$ and boson mode momentum $q=\pi$, $2\pi/3$, $2\pi/4$ and $2\pi/5$ (see text for details). Straight lines show the expected strong-coupling limits. (d) Ratio of HIC bipolaron effective total mass to twice the polaron mass. In all cases $\Omega = 0.5t$.

given above, or, more appropriately, to use weak-coupling perturbation theory.

A remarkable consequence of eq. (13) is that it gives a strong-coupling HIC polaron effective mass

$$\frac{m_P}{m} = \frac{1}{\exp\left(-\frac{2dt\lambda}{\Omega}\right) + \frac{1}{2\lambda} + \cdots} \xrightarrow{\lambda \to \infty} 2\lambda,$$

where $m = \hbar^2(2ta^2)^{-1}$ is the free electron mass. In contrast, for the Holstein polaron the first-order contribution to the analog of eq. (13) dominates the second-order contribution at strong coupling, and as a result the Holstein polaron effective mass is $m_P/m \to \exp(2dt\lambda/\Omega)$ [20]. These predictions are verified in figs. 4(a) and (b), for $d=1$ and $d=2$, which show a linear as opposed to an exponential dependence on λ for the effective mass of the HIC polaron. As a result, the HIC polaron remains rather light even for couplings where the Holstein polaron is orders of magnitude heavier than the free electron.

Another significant difference appears with respect to the isotope effect (dependence on the nuclear mass M of the atoms that constitute the lattice). It is straightforward to verify that the effective coupling λ is independent of M [22], and of course, so is the free electron mass and bandwidth. It follows that the HIC polaron mass exhibits no isotope effect (IE) at strong coupling, whereas the Holstein polaron mass has a significant IE,

$m_P \sim \exp(\sqrt{M})$, because the phonon frequency that appears in the exponent is $\Omega \sim 1/\sqrt{M}$.

In general, the renormalized mass m^* can be expressed in terms of derivatives of the self-energy [1],

$$\frac{m^*}{m} = \left(1 - \frac{\partial \Sigma}{\partial \omega}\right) \cdot \left(1 + \frac{m}{\hbar^2}\frac{\partial^2 \Sigma}{\partial k^2}\right)^{-1},$$

where all the derivatives are evaluated for $\vec{k}=0$ and at the GS energy $\omega = E_{GS}$. The first term is linked to the qp weight since $Z = (1 - \frac{\partial \Sigma}{\partial \omega})^{-1}$. As shown in fig. 1(a), the qp weights are rather similar for the two models, therefore so is this part of the contribution to the effective mass. The major difference comes from the second factor. The Holstein self-energy has rather weak $\vec{k}$-dependence, and this term contributes 20% or less to m^* [23]. In contrast, the HIC self-energy is strongly $\vec{k}$-dependent, resulting in a significantly reduced effective mass. Using strong-coupling perturbation for a $\vec{q}$-dependent coupling $g_{\vec{q}}$, we find that $m_P \sim \exp(\delta g^2/\Omega^2)$, where $\delta g^2 = \frac{1}{N}\sum_{\vec{q}}|g_{\vec{q}}|^2[1 - \cos(2q_x a)]$ for a $g_{\vec{q}}$ with cubic symmetry. For the Holstein model the second term integrates to zero, hence the heavy polaron. For the HIC model, the two terms exactly cancel out and the mass enhancement is not exponential. (Note that this is no longer true for a coupling $g_{\vec{q}}$ peaked at $\vec{Q}$ but with a finite support around $\vec{q}=\vec{Q}$. In this case, the polaron mass will acquire exponential dependence on λ, but with a very small prefactor. As a result, one still expects significantly lighter polarons than for the Holstein model, though the precise values will depend on the particular details of the model of interest).

The same cancelation of the two terms also appears for a HIC coupling strongly peaked at $\vec{q}=0$, $g_{\vec{q}} \sim \delta_{\vec{q},0}$, suggesting a light polaron as well. In fact, in this case we have $\hat{V} \sim \sum_{k\sigma} c_{\vec{k}\sigma}^\dagger c_{\vec{k}\sigma}(b_0^\dagger + b_0) \equiv N(b_0^\dagger + b_0)$, where N is the number of electrons. This term simply shifts the overall energies but leaves the electron mass unchanged. Again, one expects lighter (than Holstein) polarons if the coupling is peaked at $\vec{q}=0$ but also has support at finite $\vec{q}$. This has indeed been confirmed, for example in refs. [24,25] for the Fröhlich polaron.

In the limit $\lambda = \infty$ ($t=0$), the ground state of the HIC model can be calculated easily to be given by $|GS\rangle \propto c_i^\dagger \exp[-(g/\sqrt{N}\Omega)\sum_j (-1)^{i-j} b_j^\dagger]|0\rangle$, i.e. coherent polaron clouds form at all lattice sites, with staggered displacements $\langle GS|b_j^\dagger + b_j|GS\rangle \propto (-1)^{i-j}(2g/\sqrt{N}\Omega)$. This staggering explains the doubled unit cell in this limit. It also shows that despite the agreement in energy and qp weight with the strong-coupling Holstein polaron, the HIC polaron is very different in that it has an infinite-size phonon cloud (for $\lambda \to \infty$, the Holstein polaron's cloud is limited to the one site where the electron is located).

This provides us with another explanation of the light mass of the HIC polarons: since the energy of the electron is independent of its location inside this infinite-size phonon cloud, it is free to move on its self-defined sublattice, tunneling through sites on the other sublattice.

The effective hopping is expected to be $t^* \sim t^2/E_P$ (the height of the tunneling barrier is $\sim E_P = g^2/\Omega$) and so $m^*/m \sim t/t^* \sim \lambda$. This can be generalized to HIC coupling to a boson with momentum $\vec{q} \neq \vec{Q}$ or 0, which can also be treated exactly. In 1D there are now two distinct phonon modes to be considered, since now $b_q \neq b_{-q}$. The HIC phonon cloud in the strong coupling limit will again be infinite in size, since the GS is a coherent state involving $b_{\vec{q}}^\dagger$ and $b_{-\vec{q}}^\dagger$ bosons. For $\lambda \to \infty$ and $q = 2\pi/n$, $n = 3, 4, \ldots$, the electron now has to tunnel through $n-1$ sites before it arrives back to its original (favorable) sublattice. As a result, one now expects $t^* \sim t^n/E_P^{n-1}$ and therefore $m^*/m \sim \lambda^{n-1}$. This is indeed verified by the exact solution, as shown in fig. 4(c) for $n = 3$, 4 and 5 and $d = 1$. The same is expected to also hold for $d > 1$.

Thus, the light HIC polaron masses (in particular, the one for the $\vec{q} = \vec{Q}$ HIC model) is directly due to the infinite spatial range of the HIC model coupling. As discussed above, for long but finite-range coupling (g_q strongly peaked near $\vec{Q}$) we expect a large but finite-size phonon cloud, and a polaron much lighter than for a short-range coupling which results in a localized phonon cloud. This is consistent with earlier work showing that the increase of the electron-phonon interaction range can considerably lower the polaron mass [26–28].

HIC bipolarons are also light (see fig. 4(d)) for the same reasons. If $\lambda \to 0$, the phonon-induced interactions vanish and $m_{BP} = 2m_P$, as expected. For strong coupling, $m_{BP} \sim 4m_P = 8\lambda m$, whereas for the $\vec{q} = 0$ HIC model, $m_{BP} = 2m$. By contrast, the Holstein bipolaron total mass is $m_{BP} \sim \exp(2g^2/\Omega^2)$ [20]. These results suggest that for long-range interactions that are highly peaked around $\vec{Q}$, it is possible to have strongly bound yet still very light bipolarons at strong effective coupling λ. This may be of relevance for models of cuprates and manganites, although one needs to understand the effects of on-site Hubbard repulsion, etc., before this can be claimed. Such work is in progress.

In conclusion, we have derived exact polaron and bipolaron Green's functions for a model with a simplified electron-boson coupling, and showed that the resulting polarons and bipolarons remain extremely light even for very strong coupling. It is worth mentioning that a different mechanism for obtaining light polarons and bipolarons was recently presented in ref. [29], for a Fröhlich-like coupling but on a triangular lattice. In their case, the light bipolarons are due to a peculiar "crab-like" motion of the pair of electrons. These two examples suggest that other mechanisms giving rise to light polarons and bipolarons even at very strong couplings may yet be uncovered.

$* * *$

REFERENCES

[1] MAHAN G. D., *Many-Particle Physics* (Plenum, New York) 1981.
[2] HOLSTEIN T., *Ann. Phys. (N.Y.)*, **8** (1959) 325.
[3] HOLSTEIN T., *Ann. Phys. (N.Y.)*, **8** (1959) 343.
[4] FROLICH H., *Adv. Phys.*, **3** (1954) 325.
[5] RICE T. M. and SNEDDON L., *Phys. Rev. Lett.*, **47** (1981) 689.
[6] BISCHOFS I. B., KOSTUR V. N. and ALLEN P. B., *Phys. Rev. B*, **65** (2002) 115112.
[7] SZCZEPANSKI K. J. and BECKER K. W., *Z. Phys. B*, **89** (1992) 327.
[8] ROSCH O. and GUNNARSSON O., *Phys. Rev. Lett.*, **92** (2004) 146403.
[9] LANZARA A. *et al.*, *Nature (London)*, **412** (2001) 510.
[10] SHEN K. M. *et al.*, *Phys. Rev. Lett.*, **93** (2004) 267002.
[11] LIU Z. and MANOUSAKIS E., *Phys. Rev. B*, **45** (1992) 2425.
[12] BALA J., SAWATZKY G. A., OLES A. M. and MACRIDIN A., *Phys. Rev. Lett.*, **87** (2001) 067204.
[13] TOKURA Y. and NAGAOSA N., *Science*, **288** (2000) 462.
[14] PEREBEINOS V., TERSOFF J. and AVOURIS P., *Phys. Rev. Lett.*, **94** (2005) 086802.
[15] PUPILLO G., GRIESSNER A., MICHELI A., ORTNER M., WANG D.-P. and ZOLLER P., unpublished, arXiv:0709.1825.
[16] VISWANATH V. S. and MÜLLER G., *The Recursion Method* (Springer-Verlag, Berlin) 1994.
[17] DAMASCELLI A., HUSSAIN Z. and SHEN Z.-X., *Rev. Mod. Phys.*, **75** (2003) 473.
[18] BERCIU M., *Phys. Rev. Lett.*, **97** (2006) 036402.
[19] GOODVIN G. L., BERCIU M. and SAWATZKY G. A., *Phys. Rev. B*, **74** (2006) 245104.
[20] ALEXANDROV A. S., *Theory of Superconductivity: From Weak to Strong Coupling* (IoP Publishing, Bristol) 2003.
[21] At strong couplings, there are actually two discrete *qp* states below the first continuum in the Holstein polaron spectrum; see, for instance, BONCA J., TRUGMAN S. A. and BATISTIC I., *Phys. Rev. B*, **60** (1999) 1633; BERCIU M. and GOODVIN G. L., *Phys. Rev. B*, **76** (2007) 165109.
[22] MISHCHENKO A. S. and NAGAOSA N., *Phys. Rev. B*, **73** (2006) 092502.
[23] KU L.-C., TRUGMAN S. A. and BONCA J., *Phys. Rev. B*, **65** (2002) 174306.
[24] ALEXANDROV A. S. and BRATKOVSKY A. M., *J. Phys.: Condens. Matter*, **11** (1999) L531.
[25] ALEXANDROV A. S. and KORNILOVITCH P. E., *J. Phys.: Condens. Matter*, **14** (2002) 5337.
[26] ALEXANDROV A. S. and KORNILOVITCH P. E., *Phys. Rev. Lett.*, **82** (1999) 807.
[27] FEHSKE H., LOOS J. and WELLEIN G., *Phys. Rev. B*, **61** (2000) 8016.
[28] DE FILIPPIS G., CATAUDELLA V., MISHCHENKO A. S. and NAGAOSA N., *Phys. Rev. Lett.*, **99** (2007) 146405.
[29] HAGUE J. P., KORNILOVITCH P. E., SAMSON J. H. and ALEXANDROV A. S., *Phys. Rev. Lett.*, **98** (2007) 037002.